Hindawi
International Journal of Polymer Science
Volume 2022, Article ID 4521937, 10 pages
https://doi.org/10.1155/2022/4521937

Research Article

Biocompatible and Electroconductive Nanocomposite Scaffolds with Improved Piezoelectric Response for Bone Tissue Engineering

Sana Por Hajrezaei,[1] Masoumeh Haghbin Nazarpak,[2] Shahriar Hojjati Emami,[1] and Elham Shahryari[2]

[1]*Center of Excellence in Biomaterials, Department of Biomedical Engineering, Amirkabir University of Technology, Tehran, Iran*
[2]*New Technologies Research Center, Amirkabir University of Technology, Tehran 15875-4413, Iran*

Correspondence should be addressed to Masoumeh Haghbin Nazarpak; haghbin@aut.ac.ir
and Shahriar Hojjati Emami; semami@aut.ac.ir

Received 3 August 2021; Revised 11 January 2022; Accepted 24 March 2022; Published 25 April 2022

Academic Editor: Marta Fernández-García

Electroactive scaffolds are relatively new tools in tissue engineering that open new avenue in repairing damaged soft and hard tissues. These scaffolds can induce electrical signaling while providing an ECM-like microenvironment. However, low biocompatibility and lack of biodegradability of piezoelectric and conductive polymers limits their clinical translation. In the current study, we have developed highly biocompatible, electroconductive nanofibrous scaffolds based on poly-L-lactic acid/polyaniline/carbon nanotube (PLLA/polyaniline/CNT). Physical and chemical properties of fabricated scaffolds were tested using various techniques. Biological characteristics of the scaffolds are also examined to check cellular attachment as well as differentiation of cultured (progenitor) cells. Scaffolds were optimized to direct osteogenic differentiation of mesenchymal stem cells. Such scaffolds can offer new strategies for the regeneration of damaged/lost bone.

1. Introduction

Bone loss and damage due to injury or disease are an unmet but very significant medical issue. Due to the complexity of physiological and anatomical features of bone tissues, current standard of cares often offers low yield solutions which resulted in limited healing in the case of large-area bone defects [1]. For example, skeletal reconstruction of large-area bone defects created by infection, trauma, and tumor removal is usually fall beyond the normal healing potential [2]. Even in case of tibia fractures, it has been reported that more than 10% of fractures cannot be fully healed [3]. Bone tissue engineering offers a promising alternative strategy of healing severe bone injuries by utilizing the body's natural biological response to tissue damage in conjunction with engineering toolbox. Osteogenic cells, growth factors, and biomaterial scaffolds form the foundation of the many bone tissue engineering strategies employed to achieve repair and restoration of damaged tissue. An ideal biomaterial scaffold will provide mechanical support to an injured site and also deliver growth factors and progenitor cells into a defect to promote tissue growth. Additionally, this biomaterial should degrade in a controlled manner without causing a significant inflammatory response [4]. Such engineered biomaterial can offer promising alternative strategies of healing severe bone injuries [5]. Bone is a dynamic tissue and due to its intrinsic piezoelectric nature can convert mechanical stimuli into electrical messages [6, 7]. These piezoelectric properties can affect various cellular functions as the generated electromechanical signals can be transmitted to cells through the extracellular matrix (ECM), thereby influence matrix secretion, cell growth, and alter tissue repair [8]. Piezoelectricity plays an important role in tissue repair and regeneration through specific molecular and cellular pathways. Piezoelectric materials are a class of smart materials that can generate electrical signals in response to the applied stress. Use of

such materials for tissue engineering application also reported in the recent years [9], as these materials can potentially trigger the signaling pathways and thereby enhance the tissue regeneration process at the impaired sites [10]. Although piezoelectric ceramics have a higher piezoelectric constant, their high brittleness and slow degradation rate have limited their use as tissue engineering scaffolds. Piezoelectric polymers have many advantages over piezoceramics, including but not limited to better biocompatibility, and tunable biodegradation properties as well as easier fabrication process. So far, polyvinylidene fluoride (PVDF) was the major candidate due to its excellent piezoelectric properties. However, as PVDF offers a temporary piezoelectric dipole [11], it should be coupled with other polymers or ceramics to enter the beta phase and exhibit piezoelectric behavior before use. This factor, along with the low biocompatibility of PVDF, has limited its use as an engineered piezoelectric scaffold for medical applications [12–16].

Due to limitation of polymers with intrinsic piezoelectric properties, we have decided to fabricate the composite scaffolds not to offer the piezoelectric proptranstranstrtrerties but also to be optimized for biomedical applications. As a choice of matrix, poly (lactic acid) (PLLA) was selected as it is one of the most popular polymers which has been approved by the US Food and Drug Administration (FDA) for various medical applications due to its excellent biocompatibility and tunable biodegradability. However, the piezoelectric properties of PLLA have been less studied. The intrinsic piezoelectric property of PLLA came from the rotation of the plate defined by the CO and C = O bonds. Such a rotation results in a permanent electric dipole which make the structure able to generate electrical signals without the need of an external electrical stimulus, unlike PVDF. Such a signal can be sensed by the cells and trigger intracellular pathways to tune the cellular fate including cellular adhesion, movement, proliferation, and differentiation. Also, the use of PLLA as a material scaffold is much more cost-effective than PVDF for translational medicine [10, 17, 18]. Moreover, weaker piezoelectric properties of PLLA compared to other piezoelectric polymers can be improved by presence of conductive ingredients [6].

Rather than choice of polymers, form factor is known to affect biological outcome of biomaterial scaffolds. For example, it has been reported that the use of foam based on PLLA is problematic due to its brittleness and also the need for poststretching process. Electrospinning can be utilized as an alternative fabrication process [19]. The electrospinning is a well-known technique that can create micro/nanoscale fibers with interconnected porosity, which mimics the natural ECM of bone tissue [20–23]. Nanofibers could provide an engineered 3D support to positively affect cellular behavior such as their orientation, proliferation, migration, and function [24]. In recent years, PLLA electrospun nanofibers have been studied extensively thanks to their tunable physicochemical properties as well as promising biological outcomes in the content of bone tissue engineering [19, 25–27]. Electrospinning process can also induce piezoelectricity due to increasing the specific surface area and also by providing polymer chain tension and increasing in polarity within the structure which elevating the surface load and surface charge and consequently improving the piezoelectricity of the structure [10, 28].

On the other hand, electroconductive materials have recently been widely used in tissue engineering applications [29–31]. These materials can conduct electrical signals to the cultured cells in order to alter cellular adhesion, growth, and differentiation which can ultimately affect repair of lost tissue. Among the conductive polymers, polyaniline (PANI) seems very attractive due to its ease of synthesis and high biocompatibility [11]. According to the reports, PANI composite PLLA nanofiber scaffolds act as a suitable option for active bone tissue engineering scaffolds [30, 32, 33]. Moreover, presence of carbon nanotubes (CNT) can significantly improve the electrochemical properties of polymer-based scaffolds due to its excellent electrical properties [34, 35] and acceptable biocompatibility [36]. In this study, we have developed series of composite electrospun scaffolds with piezoelectric properties based on PLLA polymer and PANI/CNT conductive ingredients for potential bone tissue engineering applications. Physicochemical properties of fabricated scaffolds were tested using various techniques. Biological behavior of these scaffolds were tested using two distinguished and well-studied cell types to confirm the in vitro biocompatibility of designed formulations. We also demonstrate how these materials can be utilized to direct osteogenic differentiation of human mesenchymal stem cells.

2. Materials and Methods

2.1. Chemicals. Unless noted otherwise, all chemicals including poly-L-lactic acid, aniline, carbon nanotube (CNT), and MTT (3-(4, 5-dimethylthiazol-2-yl)-2, 5-diphenyltetrazolium bromide) were bought from Sigma-Aldrich, Inc. L929 (NCBI C161) cell line as well as human bone-marrow mesenchymal stem cells (hBMMSCs) were provided from Pasteur Cell Bank of Iran (PCBI).

2.2. Preparation of Nanofibrous Nanofiber Scaffolds (PLLA, PLLA/PANI, PLLA/PANI/CNT). To fabricate PLLA scaffolds, PLLA firstly was dissolved in chloroform at a concentration of 4% w/v solution, and then DMF (1 : 4 v/v DMF/chloroform) was added to the solution. The mixture stirred for 30 min before being loaded in 10 ml syringes with a 20 G needle. The solution was electrospun using a laboratory-made electrospinning device at a 14 kV at the constant infusion rate of 0.5 $ml \cdot h^{-1}$. Here, the collector to needle distance was fixed at 20 cm and collector rotated at 850 rpm to increase the surface area of collected mats. Nanofibers were collected on a device collector covered with aluminum foil and then placed in a vacuum for 48 h to remove the remining of chloroform and DMF solvents. Next, these electrospun nanofiber scaffolds were cut to specific dimensions of 1 × 1 cm and used it for further chemical and cellular tests.

Following fabrication of PLLA nanofiber mats, PANI was deposited on PLLA surface using in situ polymerization to form PLLA/PANI samples. Aniline was used as a

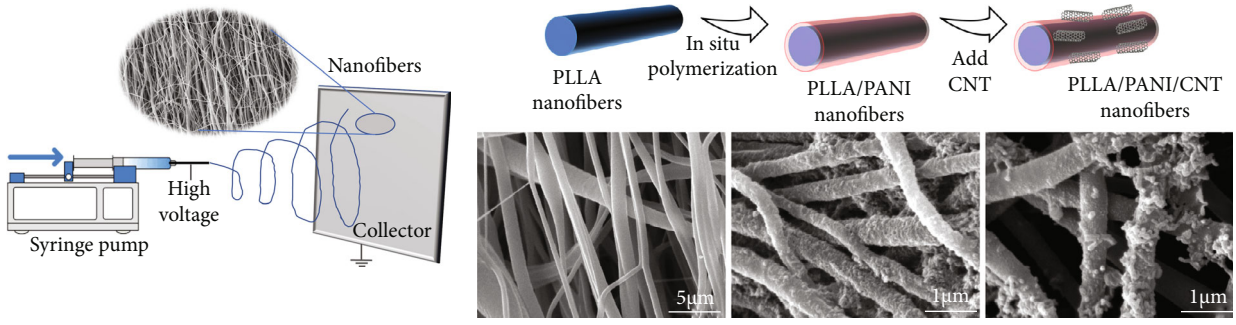

Figure 1: (a) Schematic representation of electrospinning process used to fabricate PLLA nanofibers. (b) Surface of PLLA nanofibers were modified using in situ polymerization technique to form PANI coating. Surface coating of PLLA nanofibers with PANI was also tried in the presence of CNT. Scanning electron micrographs of PLLA, PLLA/PANI, and PLLA/PANI/CNT nanofibers were presented.

monomer and ammonium persulfate (APS) as an oxidant, and the reaction was perfumed in 1 M HCl. Aniline (400 mM) was dissolved in HCl (1 M), and then PLLA nanofibers were immersed in it. Aqueous APS solution was added to the solution to initiate the polymerization reaction. The reaction was performed for 4 h in ice water bath while being stirred the stirrer. Finally, the surface coated scaffolds were washed with deionized water three times and then vacuum dried at 40°C. The samples were irradiated with UV lamp for sterilization for 2 min and stored under nitrogen atmosphere before further use. In order to incorporate CNT to the formulation to form PLLA/PANI/CNT samples, CNT at 10 wt% concentration was added to the reaction solution following the PANI deposition as mentioned earlier.

2.3. Characterization. Scanning electron microscopy (SEM; AIS2100, Seron Technology, Korea) was used to evaluate the morphology of PLLA nanofibers, PLLA/PANI, and PLLA/PANI/CNT nanofiber composites. All specimens were sputter coated with gold before imaging. Nanofiber diameters were evaluated using ImageJ software.

To characterize the molecular composition of the nanofibers, Fourier transform infrared (FTIR) spectra of PLLA, PLLA/PANI, and PLLA/PANI/CNT nanofiber mats were recorded using Perkin-Elmer FT-IR spectrophotometer (500–4000 cm^{-1}) following preparation of KBr pellets.

The conductivity meter (Keithley 1602A) was used to measure the electrical conductivity of PLLA nanofibers, PLLA/PANI, and PLLA/PANI/CNT nanofibrous composites. All samples were prepared in 1 × 1 cm dimensions and placed between two conductive probes. Following applying the electrical voltage, the output current was measured, and voltage current plots were obtained for each sample. The slope of these plots indicates the electrical conductivity of the samples.

The piezoelectric sensitivity of all three samples was measured using an oscilloscope attached to a handmade piezoelectric device (Functional Fibrous Material Research Lab, Amirkabir University of Technology, Iran) with a force frequency of 5 Hz. The amplification factor of load cell set in 500 and amplification factor of the output set in 1000. Electrical sensitivity of samples was calculated as reported in Sorayani et al. [37].

In the present study, L929 cell (NCBI C161) was used to study attachment and proliferation of model cells on designed scaffolds. Following cellular incubation, culture media exchanged every three days. Dimethylthiazol diphenyltetrazolium bromide test (MTT) was used to estimate cellular proliferation and viability over time.

Here, to evaluate the cell proliferation, 1×10^4 cells were poured onto scaffold samples with dimensions of 1 × 1 cm placed in 24-well cell culture plates. Three and five days following culture, supernatants were isolated, and MTT reagent (0.5 mg/ml) was added to each well and incubated for 4 h. The supernatants were removed, and the crystals were dissolved before being read using ELISA plate reader device (STAT FAX 2100, USA) at 570 nm.

Cellular toxicity and viability were calculated using following formula:

$$Toxicity\% = (1 - (mean\ OD\ of\ sample)/(mean\ OD\ of\ control)) \times 100, \quad (1)$$

$$\text{Viability\%} = 100 - \text{Toxicity\%}. \quad (2)$$

To evaluate cell adhesion, sterilized samples were placed in 24-well plates. Then, 3×10^4 cells in 50 μl were poured on each sample and incubated for 5 h following addition of culture medium including 10% FBS. After 24 h and 48 h, the culture medium was removed from the samples and washed with PBS for 30 s, and then the cells were fixed using glutaraldehyde (3.5 wt%). Samples were then dehydrated using sequential incubation in ethanol solutions (50%, 60%, 70%, 80%, and 95%). Samples were then dried in desiccator prior to being imaged by SEM.

To study in vitro differentiation of stem cells on surface of designed scaffolds, 1×10^6 hBMMSCs were cultured on scaffolds with various formulations in osteogenic media containing 2 mM b-glycerophosphate, 100 mM l-ascorbic acid 2-phosphate, and 10 nM dexamethasone. After 4 weeks of osteogenic induction, the cultures were stained with xylenol orange.

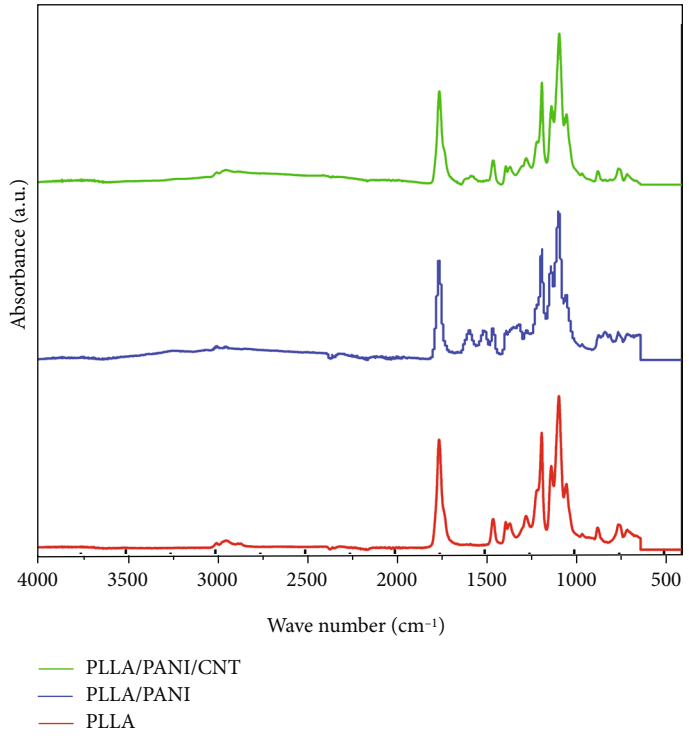

Figure 2: FTIR spectra of PLLA, PLLA/PANI, and PLLA/PANI/CNT composite nanofibers.

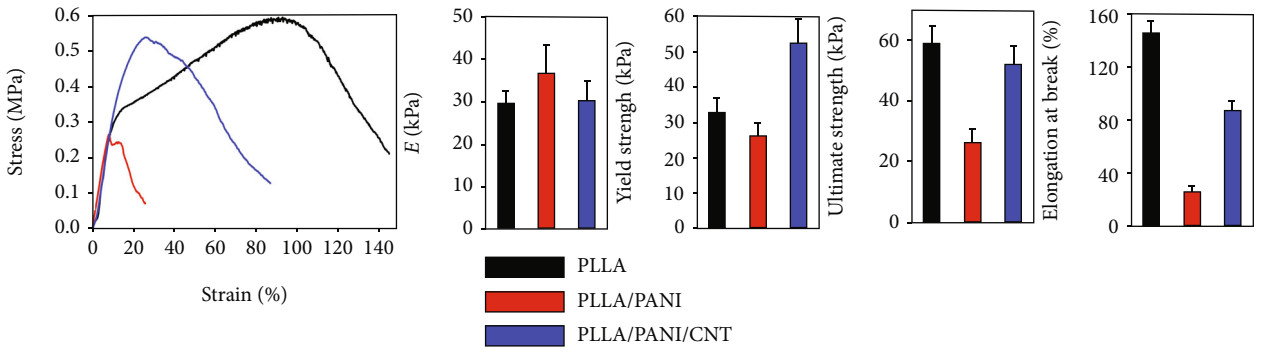

Figure 3: Stress-strain curves for PLLA (in Black), PLLA/PANI (in red) and PLLA/PANI/CNT (in blue). Elastic modulus, E, yield strength, ultimate strength, and elongation at break were calculated for mentioned samples. Black: PLLA, red: PLLA/PANI, and blue: PLLA/PANI/CNT samples. The presented data are expressed as mean ± SD ($n = 3$).

Here, ultrasound was used to stimulate the piezoelectric effect. The cells were stimulated by ultrasound four times a day during the four weeks of culture for three cycles of 10 s with 1 min delay using an laboratory scale ultrasonic bath with frequency of 100 Hz and power of 0.8 W/cm^2.

Quantitative real-time PCR assays were used to analyze the gene expression. Cultured hBMMSCs were recovered from nanofibrous scaffolds four weeks following the treatment, and RNA was isolated via TRIzol Reagent. The RNA levels of alpha l chain of collagen type I (COL1A1), core-binding factor alpha l (cbfa1), alkaline phosphatase (ALP), and osteocalcin (OCN) were reverse-transcribed, and single-stranded cDNA was made using Superscript III cDNA synthesis kits. The relative gene expression was determined using the $2^{-\Delta\Delta Ct}$ technique, normalizing to the Ct of the reference gene, glyceraldehyde-3-phosphate dehydrogenase (GAPDH): TGT TCC TAC CCC CAA TGT ATC CG-30 and 50-TGC TTC ACC ACC TTC TTG ATG TCA T.

2.4. Statistical Analysis. The Kruskal-Wallis rank sum test, one-way ANOVA, and two-tailed Student's t-test were utilized as appropriate to analyze the data at a significance of α or $p < 0.05$. Quantitative data were expressed as mean ± standard deviation (SD). For all the tests, the threshold was set to $p < 0.05$ for "statistically significant," $p < 0.01$ for "statistically very significant," and $p < 0.001$ for "statistically extremely significant." Here, all experimental were performed in triplicate with sample size of 3-5.

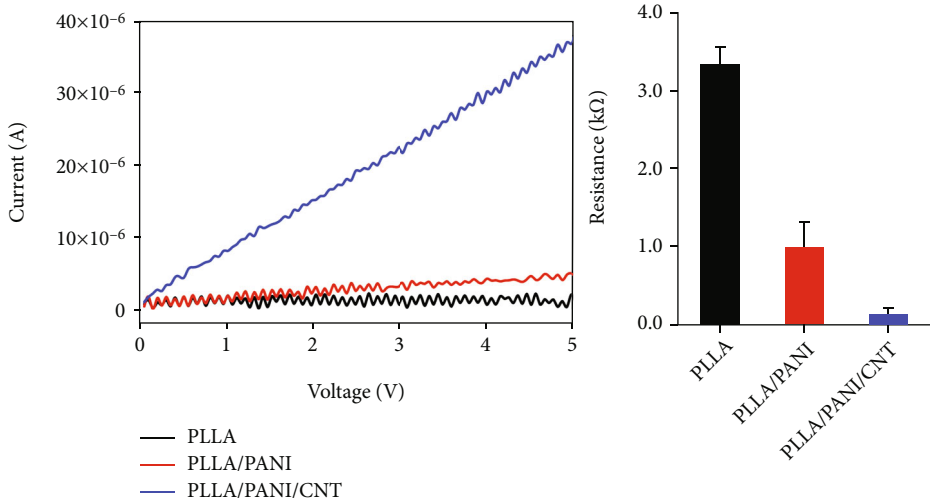

Figure 4: Current-voltage plots recorded for PLLA, PLLA/PANI/CNT, and PLLA/PANI-based nanofiber scaffolds. Electrical resistance is also calculated and plotted. The presented data are expressed as mean ± SD ($n = 3$).

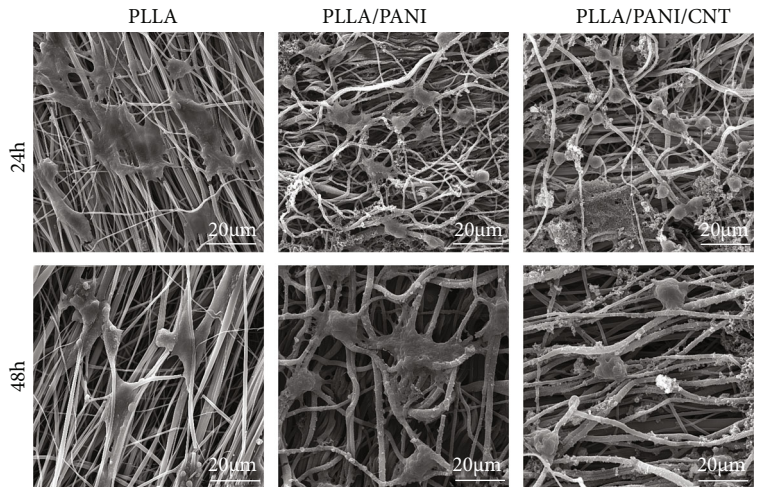

Figure 5: Scanning electron micrographs of L929 fibroblast cells cultured on PLLA, PLLA/PANI, and PLLA/PANI/CNT nanofibers at 24 and 48 timepoints.

3. Results and Discussion

Here, we first fabricate nanofiber scaffolds based on PLLA and then modified their surfaces with PANI and CNTs using in situ polymerization (Figure 1). The process of electrospinning requires an optimization of various parameters, including the voltage, the distance between the tip of the needle and the collector, and the concentration of polymer(s), flow rate, etc., to obtain uniform nanofibers. Figure 1(b) shows morphology of PLLA nanofibers with average diameter of 456 ± 4.6 nm. These beadless nanofibers have smooth surfaces with interconnected pores.

To modify piezoelectrical properties of the scaffolds, we intended to include PANI and CNT into the structure. Low miscibility of CNT with PLLA solution was identified as a limiting factor for the electrospinning method [34]. In this study, first PLLA nanofibers were fabricated by and then placed in a solution containing CNT. CNT was deposited on the surface of PLLA nanofibers through in situ polymerization of aniline as a monomer and ammonium persulfate (APS) as an oxidant. Figure 1(b) also represents the morphologies of nanofiber scaffolds of PLLA/PANI and PLLA/PANI/CNT nanofibers. According to the images obtained from scanning electron microscopy, all nanofibers have random orientation. Inclusion of PANI and CNT not only affects the surface smoothness of the fibers but also significantly ($p < 0.05$) increases the thickness of nanofibers to 675 ± 5.3 nm and 761 ± 5.2 nm for PLLA/PANI and PLLA/PANI/CNT samples, respectively.

FTIR spectrum was used to analyze changes in chemical structure of nanofibers by comparing the structure of PLLA nanofibers before and after the addition of PANI to nanofibrous PLLA. The spectrum of PLLA, PLLA/PANI, and PLLA/PANI/CNT is shown in Figure 2. Peak at 1754 cm^{-1}

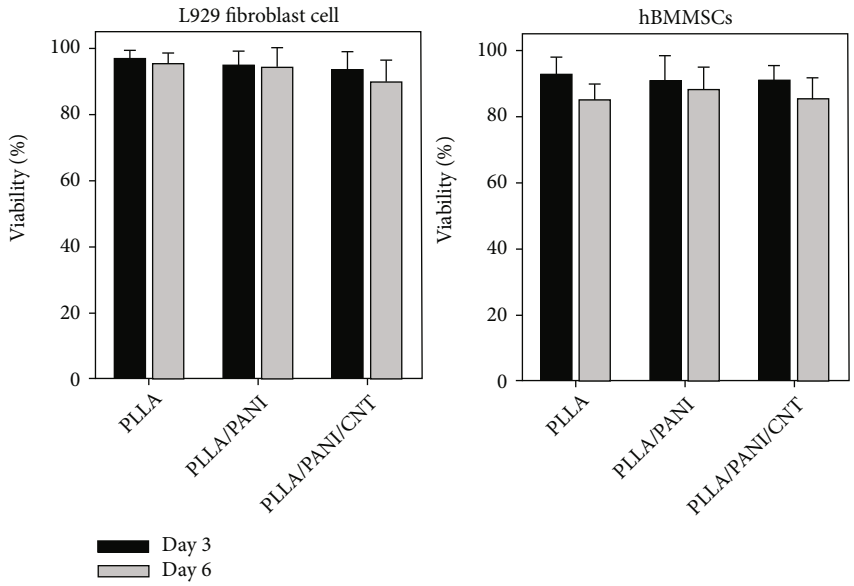

Figure 6: The viability of fibroblasts and human bone-marrow mesenchymal stem cells (hBMMSCs) on PLLA, PLLA/PANI, and PLLA/PANI/CNT nanofibrous scaffolds after being cultured for 3 and 6 days. The presented data are expressed as mean ± SD ($n = 3$).

represents the vibration of C=O bond in PLLA microstructure which is partly responsible for its piezoelectric properties. This peak remains constant across the samples. Presence of PANI is confirmed by observation of a new peak at 1586 cm^{-1}. FTIR spectra PLLA/PANI depicted all the characteristic bands of the PLLA. PANI demonstrates peaks at 3320 cm−1 which is attributed to primary amine stretching mode. The bands of 1381 cm^{-1} correspond to the C-N stretching of the secondary aromatic amine of PANI. In addition, the peak at 1586 cm−1 confirms the existence of a protonated imine, and the band characteristic of conducting protonated form is observed at 1507 cm−1 as reported before [38]. It is important to note that other bonds of PLLA/PANI were overlapped with the sharp PANI bonds. In the presence of CNT, the new peak at 1267 cm−1 is appeared which is consistent with the presence of intercalated nitrogen atoms between the graphite within carbon nanotube walls [39, 40]. In both spectra of PLLA/PANI and PLLA/PANI/CNT peaks related to PLLA are fully observed and because the piezoelectric property of the polymer PLLA is related to its inherent chemical composition, so the addition of PANI and CNT does not disturb the structure of this polymer [30]. The addition of CNT increased the intensity of piezoelectric characteristics of samples. Therefore, adding PANI/CNT to the PLLA can maintain its piezoelectric properties without making any major changes in the structure of the polymer [41–43].

To test the stability of formed coating, we have used fluorescently labeled CNT and mixed it with unmodified CNT (1 : 100 ratio). The release of labeled CNT was assessed for 14 days. Results showed less than 12% of release of CNT which unveil the strong bounding of CNT to the surface of nanofibers.

The deformation of a material in response to a load provides information about its tensile properties which affect the biological outcome of such a scaffold. Figure 3 shows the stress-strain diagram of the specimens, based on which Young's modulus was calculated. All samples demonstrated similar Young's modulus. Elastic nature of CNT strengthens the scaffolds' mechanics as reflected by increase in yield strength. Addition of PANI as a coating layer to PLLA nanofibers decreases its toughness and makes the resulted scaffolds more brittle as demonstrated by decrease in ultimate strength and elongation at break. Ultimate tensile strength is also determined by calculating the maximum amount of stress in these curves. Such a phenomena were moderated when CNT was presented in the coating formulation.

Studies found a variety of cellular responses to electric stimulation. It has been shown that conducting polymers are inducing the osteogenic regeneration [23]. It is noticeable that successful use of electroactive polymers such as PANI in nanocomposites in biomedical applications has encouraged researchers to study new formulations for their further studies. During this study, the resistance (R) of the scaffolds was measured and drawn as a linear current-voltage curve [44]. In a line diagram, the slope indicates the amount of electrical conductivity property of PLLA, PLLA/PANI, and PLLA/PANI/CNT scaffolds presented in Figure 4. Presence of PANI reduces the resistance significantly. Similar trend has been reported before [45].

However, PLLA/PANI/CNT composite fabrication showed further increased in electrical conductivity compared to PLLA/PANI composite scaffolds due to the presence of electroactive and electroconductive CNT. Such an increase may also promote piezoelectricity of the resulted scaffolds [46].

Prepared samples are examined by PiezoTester to evaluate their performance. Piezoelectric property of the PLLA/PANI/CNT fibers (0.57 mV/N) was significantly higher than those for PLLA (0.23 mV/N) and PLLA/PANI (0.35 mV/N) samples. By modifying surface of PLLA with PANI and PANI/CNT, the piezoelectricity increased by

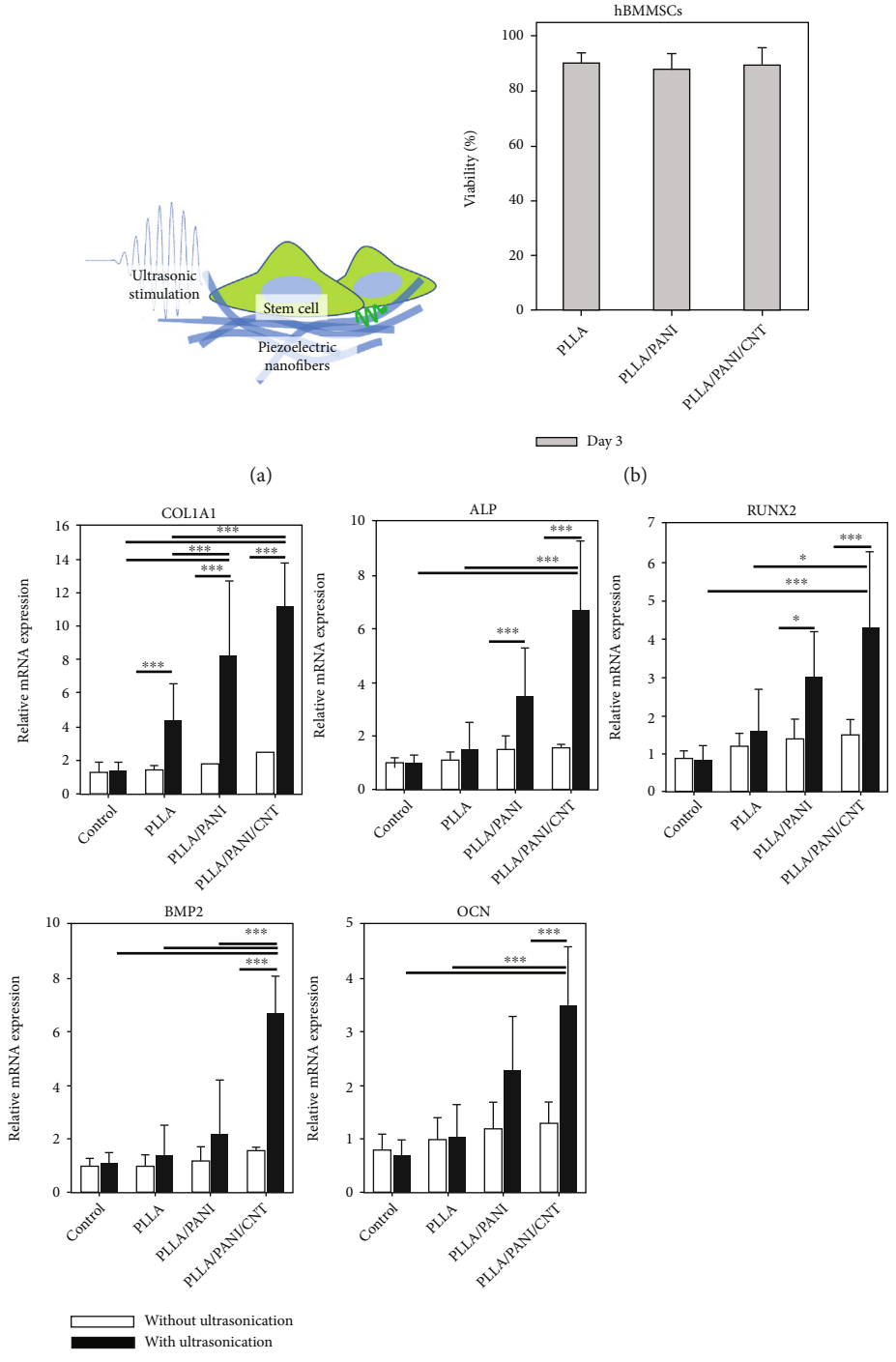

FIGURE 7: (a) Schematic representation of the ultrasound stimulation of stem cells cultured on nanofibrous scaffolds. (b) The viability of hBMMSCs on PLLA, PLLA/PANI, and PLLA/PANI/CNT nanofibrous scaffolds after being cultured for 3 in presence of ultrasound stimulation. (c) Analysis of gene expression profiles of osteogenic markers. Real-time polymerase chain reaction (qPCR) analysis of the osteogenic differentiation of hBMMSCs cultured on PLLA-based nanofibrous after 4 weeks in osteogenic media in presence or absence of external stimulation, here, ultrasolication. Expression levels of five osteogenic genes, COL1A1, BMP-2, RUNX2, BMP2, and OCN were evaluated relative to GAPDH, which was used as a housekeeping gene. The data are expressed as mean ± SD ($n = 5$). The results were statistically analyzed using one-way ANOVA with post-hoc analysis. For all the tests, the threshold was set to $p < 0.05$ for "statistically significant", $p < 0.01$ for "statistically very significant," and $p < 0.001$ for "statistically extremely significant." Statistical significance is indicated by * (significant), ** (very significant), and *** (extremely significant) for differences between samples with different formulations.

1.5- and 2.47-folds, respectively. It was reported that CNT affects the crystallinity of PLLA, and as crystallinity has a positive effect on piezoelectricity, adding CNT to the structure will improve the piezoelectricity [36]. By use of conductive elements in scaffolds, the conductivity will increase and cause induction in the piezoelectricity due to improvement of generating electrical signals in the structure. However, there are some concerns related to their toxicity and cellular response of these conductive materials that should be considered and optimized before any biomedical use.

Following the physical characterization of designed piezoelectric scaffolds, we intended to examine their biological performance. Scanning electron microscopes were used to evaluate cellular adhesion, spreading, and growth. Fibroblast attachment on the prepared scaffolds was used as an earlier step in cellular interactions, as assessed by SEM after being incubated for after 24 h and 48 h (Figure 5). SEM images revealed strong adhesion and spreading of L929 (NCBI C161) fibroblast cells to all designed scaffolds due to high surface area of nanofibrous structures after 24 and 48 h of culture. It has been reported that not only inherent toxicity of CNT will be limited at low concentration (~1 wt%) but it cans also support cell growth [41, 47–49].

Survival and cellular activity are important factors in assessing the biocompatibility of scaffolds for bone tissue engineering. Here, we examined these factors using standard MTT assay and live/dead staining. The results were compared with cells cultured on control (blank) scaffolds. As shown in Figure 6, high level of L929 cell proliferation was observed which confirms all samples are sufficiently support cellular process.

Our results also revealed over 95% viability for L929 cell and over 85% viability for hBMMSCs, 3 and 6 days after being culture on designed nanofibrous scaffolds. The lowest viability was seen for PLLA/PANI/CNT scaffolds which might be due to the presence of CNT which negatively affect the cell viability of resulted scaffolds. It has been reported that increased production of oxidants, oxidative stresses, and in the presence of CNT can cause cellular damage and lower cellular viability [50, 51].

As the proposed mechanism of action for designed scaffolds is via their piezoelectric effect, in this work, the ultrasound is selected as an external stimulation to trigger the piezoelectric effect through scaffolds during cell culture (Figure 7(a)) [52–54]. Due to the deep penetration of ultrasound waves in human tissues, such stimulation can be implemented into the clinical practices. The cells were stimulated by ultrasound four times a day for 30 s within an ultrasonic bath. Similar treatment strategy has been reported before [54].

After culturing cells in osteogenic media for one and four weeks in presence or absence of ultrasound stimulation, cells were isolated from the scaffolds. Such a treatment will not affect the viability of cultured hBMMSCs (Figure 7(b)).

Quantitative polymerase chain reaction (qPCR) was used to investigate the expression level of BMP2 as well as various osteoblastic markers including alkaline phosphatase (ALP), runt-related transcription factor2 (RUNX2), osteocalcin (OCN), and alpha-1 type I collagen (COL1A1) after one and four weeks of culturing cells (Figure 7(c)).

A significant increase (>6 folds) was observed in BMP2 expression level while having CNT and PANI into the formulation. Higher expression levels of other osteogenic markers also demonstrated. For example, a higher expression of ALP, which has a critical role in the initiation of mineralization, was observed for PANI and PANI/CNT coated samples four weeks postculture. Higher expression of other early osteogenic markers including COL1A1 and RUNX2 also observed for these samples. Besides, qPCR data show significantly higher expression of late-stage osteogenic and bone-specific markers like OCN. This marker expressed right before and alongside during the matrix mineralization.

4. Conclusion

In this study, PLLA nanofiber scaffolds were prepared by electrospinning technique. The in situ polymerization method was used to coat the surface of fibers with PANI conductive polymer as well as CNT conductive nanostructure. The results showed enhanced electrical conductivity and electrochemical behavior of resulted nanofibrous scaffolds. These scaffolds demonstrate great potential as engineering substrates for adhesion, growth, and proliferation for fibroblasts as well as stem cells without showing any toxicity. Once being cultured in osteogenic media, human bone marrow mesenchymal stem cells cultured on PLLA/PANI/CNT piezoelectric composite scaffolds showed the highest level of osteogenic differentiation. This indicates that the addition of the conductive elements, here, PANI and CNT, in a piezoelectric structure can increased the electrical signaling between cells and induce their growth and differentiation.

Data Availability

No data were used to support this study.

Conflicts of Interest

The authors have no conflicts of interest to declare. There is no financial interest to report.

Authors' Contributions

All co-authors have seen and agreed with the contents of the manuscript.

References

[1] M. Wagh and D. Ravalia, "Bone regeneration and repair: current and future aspects," *International Journal of Science and Research (IJSR)*, vol. 4, pp. 351–355, 2015.

[2] R. Dimitriou, E. Jones, D. McGonagle, and P. V. Giannoudis, "Bone regeneration: current concepts and future directions," *BMC Medicine*, vol. 9, pp. 1–10, 2011.

[3] L. Audigé, D. Griffin, M. Bhandari, J. Kellam, and T. P. Rüedi, "Path analysis of factors for delayed healing and nonunion in 416 operatively treated tibial shaft fractures," *Clinical*

Orthopaedics and Related Research, vol. 438, no. 438, pp. 221–232, 2005.

[4] A. Malek-Khatabi, H. A. Javar, E. Dashtimoghadam, S. Ansari, M. M. Hasani-Sadrabadi, and A. Moshaverinia, "In situ bone tissue engineering using gene delivery nanocomplexes," *Acta Biomaterialia*, vol. 108, pp. 326–336, 2020.

[5] Q. Hongfei and L. Tingli, "Biomimetic hydroxyapatite-containing PLLA/PCL electrospun nanofibrous scaffold for bone tissue engineering," *Frontiers in Bioengineering and Biotechnology*, vol. 4, 2016.

[6] B. Tandon, J. J. Blaker, and S. H. Cartmell, "Piezoelectric materials as stimulatory biomedical materials and scaffolds for bone repair," *Acta Biomaterialia*, vol. 73, pp. 1–20, 2018.

[7] E. Fukada and I. Yasuda, "On the piezoelectric effect of bone," *Journal of the Physical Society of Japan*, vol. 12, no. 10, pp. 1158–1162, 1957.

[8] B. Miara, E. Rohan, M. Zidi, and B. Labat, "Piezomaterials for bone regeneration design–homogenization approach," *Journal of the Mechanics and Physics of Solids*, vol. 53, no. 11, pp. 2529–2556, 2005.

[9] C. Polley, T. Distler, R. Detsch et al., "3D printing of piezoelectric barium titanate-hydroxyapatite Scaffolds with interconnected porosity for bone tissue engineering," *Materials*, vol. 13, no. 7, p. 1773, 2020.

[10] A. S. Motamedi, H. Mirzadeh, F. Hajiesmaeilbaigi, S. Bagheri-Khoulenjani, and M. Shokrgozar, "Effect of electrospinning parameters on morphological properties of PVDF nanofibrous scaffolds," *Progress in Biomaterials*, vol. 6, no. 3, pp. 113–123, 2017.

[11] A. Mirzaei, E. Saburi, S. E. Enderami et al., "Synergistic effects of polyaniline and pulsed electromagnetic field to stem cells osteogenic differentiation on polyvinylidene fluoride scaffold," *Artificial Cells, Nanomedicine, and Biotechnology*, vol. 47, no. 1, pp. 3058–3066, 2019.

[12] H. Jiao, S. Song, K. Zhao, X. Zhang, and Y. Tang, "Synthesis and properties of porous piezoelectric BT/PHBV composite scaffold," *Journal of Biomaterials Science, Polymer Edition*, vol. 31, no. 12, pp. 1552–1565, 2020.

[13] J. Liu, H. Gu, Q. Liu, L. Ren, and G. Li, "An intelligent material for tissue reconstruction: the piezoelectric property of polycaprolactone/barium titanate composites," *Materials Letters*, vol. 236, pp. 686–689, 2019.

[14] Y. Yang, S. Peng, F. Qi et al., "Graphene-assisted barium titanate improves piezoelectric performance of biopolymer scaffold," *Materials Science and Engineering: C*, vol. 116, article 111195, 2020.

[15] A. S. Motamedi, H. Mirzadeh, F. Hajiesmaeilbaigi, S. Bagheri-Khoulenjani, and M. A. Shokrgozar, "Piezoelectric electrospun nanocomposite comprising Au NPs/PVDF for nerve tissue engineering," *Journal of Biomedical Materials Research. Part A*, vol. 105, no. 7, pp. 1984–1993, 2017.

[16] G. BaoLin and M. X. Peter, "Synthetic biodegradable functional polymers for tissue engineering: a brief review," *Science China Chemistry*, vol. 57, pp. 490–500, 2014.

[17] T. M. Raimondo and D. J. Mooney, "Functional muscle recovery with nanoparticle-directed M2 macrophage polarization in mice," *Proceedings of the National Academy of Sciences of the United States of America*, vol. 115, no. 42, pp. 10648–10653, 2018.

[18] Y. Li, C. Liao, and S. C. Tjong, "Electrospun polyvinylidene fluoride-based fibrous scaffolds with piezoelectric characteristics for bone and neural tissue engineering," *Nanomater*, vol. 9, 2019.

[19] S. J. Lee, A. P. Arun, and K. J. Kim, "Piezoelectric properties of electrospun poly(l-lactic acid) nanofiber web," *Materials Letters*, vol. 148, pp. 58–62, 2015.

[20] W. E. Teo and S. Ramakrishna, "A review on electrospinning design and nanofibre assemblies," *Nanotechnology*, vol. 17, no. 14, pp. R89–R106, 2006.

[21] A. Bagchi, S. R. K. Meka, B. N. Rao, and K. Chatterjee, "Perovskite ceramic nanoparticles in polymer composites for augmenting bone tissue regeneration," *Nanotechnology*, vol. 25, no. 48, article 485101, 2014.

[22] S. R. K. Meka, S. Kumar Verma, V. Agarwal, and K. Chatterjee, "In situ silication of polymer nanofibers to engineer multibiofunctional composites," *ChemistrySelect*, vol. 3, no. 13, pp. 3762–3773, 2018.

[23] S. R. K. Meka, V. Agarwal, and K. Chatterjee, "_In situ_ preparation of multicomponent polymer composite nanofibrous scaffolds with enhanced osteogenic and angiogenic activities," *Materials Science and Engineering: C*, vol. 94, pp. 565–579, 2019.

[24] M. F. Abazari, F. Nejati, N. Nasiri et al., "Platelet-rich plasma incorporated electrospun PVA-chitosan-HA nanofibers accelerates osteogenic differentiation and bone reconstruction," *Gene*, vol. 720, article 144096, 2019.

[25] W. Cui, L. Cheng, H. Li, Y. Zhou, Y. Zhang, and J. Chang, "Preparation of hydrophilic poly(l-lactide) electrospun fibrous scaffolds modified with chitosan for enhanced cell biocompatibility," *Polymer*, vol. 53, no. 11, pp. 2298–2305, 2012.

[26] W. Y. Lai, S. W. Feng, Y. H. Chan, W. J. Chang, H. T. Wang, and H. M. Huang, "In vivo investigation into effectiveness of Fe3O4/PLLA nanofibers for bone tissue engineering applications," *Polymers*, vol. 10, no. 7, p. 804, 2018.

[27] B. K. Gu, M. S. Kim, C. M. Kang, K. J. Il, S. J. Park, and C. H. Kim, "Fabrication of conductive polymer-based nanofiber scaffolds for tissue engineering applications," *Journal of Nanoscience and Nanotechnology*, vol. 14, no. 10, pp. 7621–7626, 2014.

[28] J. Xue, J. Xie, W. Liu, and Y. Xia, "Electrospun nanofibers: new concepts, materials, and applications," *Accounts of Chemical Research*, vol. 50, no. 8, pp. 1976–1987, 2017.

[29] B. Guo and P. X. Ma, "Conducting polymers for tissue engineering," *Biomacromolecules*, vol. 19, no. 6, pp. 1764–1782, 2018.

[30] J. Chen, M. Yu, B. Guo, P. X. Ma, and Z. Yin, "Conductive nanofibrous composite scaffolds based on _in-situ_ formed polyaniline nanoparticle and polylactide for bone regeneration," *Journal of Colloid and Interface Science*, vol. 514, pp. 517–527, 2018.

[31] L. Li, M. Yu, P. X. Ma, and B. Guo, "Electroactive degradable copolymers enhancing osteogenic differentiation from bone marrow derived mesenchymal stem cells," *Journal of Materials Chemistry B*, vol. 4, no. 3, pp. 471–481, 2016.

[32] Y. Liu, H. Cui, X. Zhuang, Y. Wei, and X. Chen, "Electrospinning of aniline pentamer-graft-gelatin/PLLA nanofibers for bone tissue engineering," *Acta Biomaterialia*, vol. 10, no. 12, pp. 5074–5080, 2014.

[33] S. Nagam Hanumantharao, C. Que, and S. Rao, "Self-assembly of 3D nanostructures in electrospun polycaprolactone-polyaniline fibers and their application as scaffolds for tissue engineering," *Materialia*, vol. 6, article 100296, 2019.

[34] M. G. Hosseini and E. Shahryari, "Fabrication of novel solid-state supercapacitor using a Nafion polymer membrane with graphene oxide/multiwalled carbon nanotube/polyaniline," *Journal of Solid State Electrochemistry*, vol. 21, no. 10, pp. 2833–2848, 2017.

[35] M. G. Hosseini and E. Shahryari, "Synthesis, characterization and electrochemical study of graphene oxide-multi walled carbon nanotube-manganese oxide-polyaniline electrode as supercapacitor," *Journal of Materials Science and Technology*, vol. 32, no. 8, pp. 763–773, 2016.

[36] G. Wang, F. Qi, W. Yang et al., "Crystallinity and reinforcement in poly-L-lactic acid scaffold induced by carbon nanotubes," *Advances in Polymer Technology*, vol. 2019, Article ID 8625325, 10 pages, 2019.

[37] M. S. Sorayani Bafqi, A. H. Sadeghi, M. Latifi, and R. Bagherzadeh, "Design and fabrication of a piezoelectric out-put evaluation system for sensitivity measurements of fibrous sensors and actuators," *Journal of Industrial Textiles*, vol. 50, no. 10, pp. 1643–1659, 2021.

[38] K. A. Ibrahim, "Synthesis and characterization of polyaniline and poly(aniline-co-o- nitroaniline) using vibrational spectroscopy," *Arabian Journal of Chemistry*, vol. 10, pp. S2668–S2674, 2017.

[39] A. Misra, P. K. Tyagi, P. Rai, and D. S. Misra, "FTIR spectroscopy of multiwalled carbon nanotubes: a simple Approachto study the nitrogen doping," *Journal of Nanoscience and Nanotechnology*, vol. 7, no. 6, pp. 1820–1823, 2007.

[40] H. C. Choi, S. Y. Bae, J. Park et al., "Experimental and theoretical studies on the structure of N-doped carbon nanotubes: possibility of intercalated molecular N2," *Applied Physics Letters*, vol. 85, no. 23, pp. 5742–5744, 2004.

[41] Q. Cheng, K. Rutledge, and E. Jabbarzadeh, "Carbon nanotube-poly(lactide-co-glycolide) composite scaffolds for bone tissue engineering applications," *Annals of Biomedical Engineering*, vol. 41, no. 5, pp. 904–916, 2013.

[42] E. Hirata, T. Akasaka, M. Uo, H. Takita, F. Watari, and A. Yokoyama, "Carbon nanotube-coating accelerated cell adhesion and proliferation on poly (L-lactide)," *Applied Surface Science*, vol. 262, pp. 24–27, 2012.

[43] G. Lekshmi, S. S. Sana, V. H. Nguyen et al., "Recent Progress in Carbon Nanotube Polymer Composites in Tissue Engineering and Regeneration," *International Journal of Molecular Sciences*, vol. 21, p. 6440, 2020.

[44] D. W. Lin, C. J. Bettinger, J. P. Ferreira, C. L. Wang, and Z. Bao, "A cell-compatible conductive film from a carbon nanotube network adsorbed on poly-L-lysine," *ACS Nano*, vol. 5, no. 12, pp. 10026–10032, 2011.

[45] F. Ghorbani, B. Ghalandari, A. L. Khan, D. Li, A. Zamanian, and B. Yu, "Decoration of electrical conductive polyurethane-polyaniline/polyvinyl alcohol matrixes with mussel-inspired polydopamine for bone tissue engineering," *Biotechnology Progress*, vol. 36, no. 6, 2020.

[46] N. Sultana, S. Bandyopadhyay-Ghosh, and C. F. Soon, "Stimulus-receptive conductive polymers for tissue engineering," in *Tissue Engineering Strategies for Organ Regeneration*, pp. 144–156, CRC Press, Boca Raton, Florida, 2020.

[47] D. Zhang, M. A. Kandadai, J. Cech, S. Roth, and S. A. Curran, "Poly(L-lactide) (PLLA)/multiwalled carbon nanotube (MWCNT) composite: characterization and biocompatibility evaluation," *The Journal of Physical Chemistry. B*, vol. 110, no. 26, pp. 12910–12915, 2006.

[48] S. Vardharajula, S. Z. Ali, P. M. Tiwari et al., "Functionalized carbon nanotubes: biomedical applications," *International Journal of Nanomedicine*, vol. 7, pp. 5361–5374, 2012.

[49] J. N. Mackle, D. J. P. Blond, E. Mooney et al., "In vitro characterization of an electroactive carbon-nanotube-based nanofiber scaffold for tissue engineering," *Macromolecular Bioscience*, vol. 11, no. 9, pp. 1272–1282, 2011.

[50] S. Pichardo, D. Gutiérrez-Praena, M. Puerto, and E. S.-T. Vitro, "Oxidative stress responses to carboxylic acid functionalized single wall carbon nanotubes on the human intestinal cell line Caco-2," *Toxicology in Vitro*, vol. 26, no. 5, pp. 672–677, 2012.

[51] L. Zhou, H. J. Forman, Y. Ge, and J. Lunec, "Multi-walled carbon nanotubes: a cytotoxicity study in relation to functionalization, dose and dispersion," *Toxicology In Vitro*, vol. 42, pp. 292–298, 2017.

[52] J. Jacob, N. More, K. Kalia, and G. Kapusetti, "Piezoelectric smart biomaterials for bone and cartilage tissue engineering," *Inflammation and Regeneration*, vol. 38, pp. 1–11, 2018.

[53] M. Hoop, X. Z. Chen, A. Ferrari et al., "Ultrasound-mediated piezoelectric differentiation of neuron-like PC12 cells on PVDF membranes," *Scientific Reports*, vol. 7, no. 1, 2017.

[54] C. Shuai, G. Liu, Y. Yang et al., "Functionalized $BaTiO_3$ enhances piezoelectric effect towards cell response of bone scaffold," *Colloids Surfaces B Biointerfaces*, vol. 185, article 110587, 2020.